Propagation of THz acoustic wave packets in GaN at room temperature

Citation: Maznev, Alexei et al. "Propagation of THz acoustic wave packets in GaN at room temperature." Applied Physics Letters, 112, 6, (February 2018): 061903 © 2018 Authors

As Published: https://doi.org/10.1063/1.5008852

Publisher: AIP Publishing LLC

Persistent URL: https://hdl.handle.net/1721.1/123669

Version: Final published version: final published article, as it appeared in a journal, conference proceedings, or other formally published context

Propagation of THz acoustic wave packets in GaN at room temperature

A. A. Maznev, T.-C. Hung, Y.-T. Yao, T.-H. Chou, J. S. Gandhi, L. Lindsay, H. D. Shin, D. W. Stokes, R. L. Forrest, A. Bensaoula, C.-K. Sun, and K. A. Nelson

Citation: Appl. Phys. Lett. **112**, 061903 (2018);

View online: https://doi.org/10.1063/1.5008852

View Table of Contents: http://aip.scitation.org/toc/apl/112/6

Published by the American Institute of Physics

Propagation of THz acoustic wave packets in GaN at room temperature

A. A. Maznev,[1,a)] T.-C. Hung,[2] Y.-T. Yao,[2] T.-H. Chou,[2] J. S. Gandhi,[3] L. Lindsay,[4] H. D. Shin,[1] D. W. Stokes,[3] R. L. Forrest,[3] A. Bensaoula,[3,b)] C.-K. Sun,[2] and K. A. Nelson[1]
[1]*Department of Chemistry, Massachusetts Institute of Technology, Cambridge, Massachusetts 02139, USA*
[2]*Graduate Institute of Photonics and Optoelectronics, National Taiwan University, Taipei 10617, Taiwan*
[3]*Department of Physics, University of Houston, Houston, Texas 77204, USA*
[4]*Materials Science and Technology Division, Oak Ridge National Laboratory, Oak Ridge, Tennessee 37831, USA*

(Received 10 October 2017; accepted 22 January 2018; published online 6 February 2018)

We use femtosecond laser pulses to generate coherent longitudinal acoustic phonons at frequencies of 1–1.4 THz and study their propagation in GaN-based structures at room temperature. Two InGaN-GaN multiple-quantum-well (MQW) structures separated by a 2.3 μm-thick GaN spacer are used to simultaneously generate phonon wave packets with a central frequency determined by the period of the MQW and detect them after passing through the spacer. The measurements provide lower bounds for phonon lifetimes in GaN, which are still significantly lower than those from first principles predictions. The material Q-factor at 1 THz is found to be at least as high as 900. The measurements also demonstrate a partial specular reflection from the free surface of GaN at 1.4 THz. This work shows the potential of laser-based methods for THz range phonon spectroscopy and the promise for extending the viable frequency range of GaN-based acousto-electronic devices. *Published by AIP Publishing.* https://doi.org/10.1063/1.5008852

Acoustic phonons with frequencies in the THz range are the dominant heat carriers in non-metallic solids at room temperature. Thermal acoustic phonons and their interactions with other phonons, boundaries, defects, and impurities have been the focus of intense efforts in studying nanoscale thermal transport in the past decade.[1] While thermal transport research deals with incoherent thermal phonon sources, the field of acoustics studies coherent acoustic waves (coherent phonons) with a well-defined absolute phase. Experiments with coherent THz phonons present many advantages for elucidating basic microscopic features of phonon transport over typical thermal conductivity studies where the information content is integrated over all phonon modes, losing important fundamental details. Indeed, the propagation of coherent THz phonon wave packets is often simulated in molecular dynamics studies.[2–4] In terms of experiments, the use of femtosecond laser pulses for generation and detection of acoustic waves[5] has ushered in acoustic measurements in the sub-THz range, which have now become routine and provide valuable insight into phonon-phonon, phonon-boundary, and electron-phonon interactions.[6–10] Progress towards THz acoustics, however, has been slow.

At 1 THz, acoustic wavelengths are typically in the single-digit nanometer range, and thus, coherent THz phonons can be easily destroyed by nanometer-scale surface or interface roughness.[7] Consequently, the most significant progress in generating THz acoustic waves has been achieved with epitaxial semiconductor structures characterized by high-quality, single-crystal layers and interfaces.[11] Typically, researchers use periodic multiple-quantum-well (MQW) structures designed in such a way that the excitation laser wavelength is absorbed in the wells but not in the barriers.[12–14] The frequency of acoustic waves generated in MQWs is determined by the periodicity of the structure, with the fundamental eigenmode frequency approximately equal to v/d, where d is the MQW period and v is the speed of sound in the MQW. In experiments with GaAs-AlAs MQWs at cryogenic temperatures ($\sim$15 K), the generation and propagation of longitudinal acoustic (LA) waves up to 1.2 THz were observed.[15,16] In a very recent study,[17] measurements of the phonon mean free path (MFP) in GaAs at frequencies up to 1 THz and temperatures 10–60 K were performed using GaAs-AlAs MQWs, offering keen insights into the physics of phonon-phonon interactions. In InGaN-GaN MQWs, coherent acoustic phonons at even higher frequencies, up to 2.5 THz, were generated at room temperature.[18,19] However, in the latter case, THz phonons were only observed in the same MQW structure where they were generated. The objective of the present work is to observe the propagation of coherent phonons in GaN above 1 THz, generated and detected at different locations within the sample at room temperature.

The choice of GaN for this study was motivated not only by the encouraging previous results on the laser generation of THz coherent phonons in GaN-based structures but also because it is an important electronic and opto-electronic material, with phonon-mediated thermal transport playing a crucial role in the thermal management of GaN-based devices.[1,20,21] Furthermore, GaN is a promising acousto-electronic material.[22] While GaN-based acousto-electronic devices currently operate at frequencies below $\sim$10 GHz, characterizing acoustic properties of GaN at higher frequencies is critical for future developments of this technology.

At ultrasonic frequencies (on the order of 1 GHz and below), the phonon MFP is inversely proportional to the frequency squared.[23,24] The longitudinal acoustic phonon lifetime in GaN at 1.2 GHz at room temperature can be obtained from a reported Q-factor of 1885 of a thin film resonator

a)Author to whom correspondence should be addressed: alexei.maznev@gmail.com
b)Present address: Institute of Physics, Academia Sinica, Taipei 11574, Taiwan

believed to be dominated by intrinsic losses in GaN.[25] This yields a lifetime of 0.25 μs, which corresponds to a MFP of 2 mm. If the quadratic dependence of the acoustic attenuation on frequency continued into the THz range, the MFP at 1.2 THz would be expected to be ~2 nm, which is smaller than the phonon wavelength (6.7 nm at this frequency). However, the quadratic dependence does not continue from GHz to THz frequencies as the phonon dissipation transitions from the Akhiezer relaxation regime at low frequencies to the Landau-Rumer (three-phonon scattering) regime at high frequencies (where the frequency dependence of the attenuation again becomes nearly quadratic).[6,9,22,26] Indeed, measurements at 435 GHz showed almost negligible attenuation of longitudinal acoustic (LA) phonons in GaN over a distance of 2 μm.[27]

On the theory side, meaningful calculations of lifetimes of THz phonons remained out of reach until recent breakthroughs in *ab-initio* calculations of anharmonic phonon interactions.[28–33] Such methods employ density functional theory (DFT)[34,35] to determine interatomic forces coupled with quantum mechanical perturbation theory (Fermi's golden rule) to determine phonon-phonon scattering probabilities.[31–33,36] The lifetime of each phonon mode is then given by the inverse of the sum of all scattering probabilities that conserve energy and crystal momentum. Figure 1 shows the dependence of the LA phonon lifetime on frequency for propagation along the *c* axis of wurtzite GaN we obtained using Eqs. (2) and (3) from Ref. 30, which give the scattering probabilities from three-phonon processes and from natural isotopic variations, respectively. (However, phonon-isotope scattering contributes less than ~1% to the total scattering rate at frequencies below 2 THz.) One can see that in the range of 1–2 THz the lifetime is expected to vary between 1 ns and 150 ps, which corresponds to a MFP range of 1.2–8 μm. Based on these theoretical predictions, we set out to observe THz phonon propagation over a few microns using two MQW structures separated by a bulk GaN spacer which are employed to simultaneously generate and detect coherent phonon wavepackets.[27]

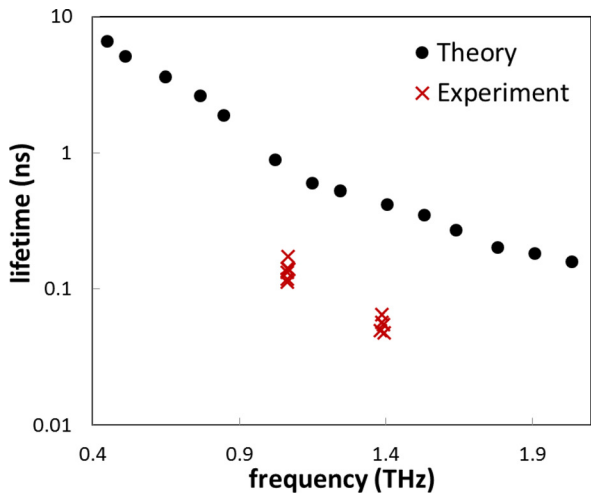

FIG. 1. *Ab-initio* longitudinal acoustic phonon lifetime vs frequency in wurtzite GaN at 300 K for the wave vector direction along the *c* axis (circles) and lower bound experimental data from the current work (crosses, each symbol corresponds to a different point on the sample).

The sample structure is schematically depicted in Fig. 2(a). $In_{0.2}Ga_{0.8}N$/GaN MQWs were grown using a custom-built molecular beam epitaxy (MBE) tool[37] on commercially available c-plane GaN templates (5 μm thick) on double-polished 300 μm-thick sapphire substrates. The growth sequence was as follows: ~50 nm GaN buffer layer, 9-period superlattice structure (MQW1) comprising $In_{0.2}Ga_{0.8}N$ quantum wells separated by GaN barrier layers, 2.3 μm GaN spacer layer, the second superlattice (MQW2) identical to MQW1, and 120 nm GaN cap layer. *In situ* reflection high energy electron diffraction (RHEED) was used to monitor the growth process. Two samples, with MQW thicknesses of 8 nm (sample 1) and 5.5 nm (sample 2), were fabricated. Figure 2(b) shows a scanning transmission electron microscopy (STEM) image of the top superlattice structure (MQW2) of sample 2, indicating excellent uniformity.

Experiments were conducted with an optical pump-probe setup based on a frequency-doubled Ti:sapphire laser with a pulse duration of ~200 fs and a repetition rate of 76 MHz. The wavelength of the pump and probe was 404 nm, corresponding to a photon energy below the bandgap of GaN but above the bandgap of $In_{0.2}Ga_{0.8}N$ quantum wells. The pulse energy and the laser spot diameter at the sample were 0.5 nJ/15 μm for pump pulses and 0.05 nJ/15 μm for probe pulses. We measured the intensity of the transmitted probe pulse as a function of its delay with respect to the pump pulse introduced by a mechanical delay line.

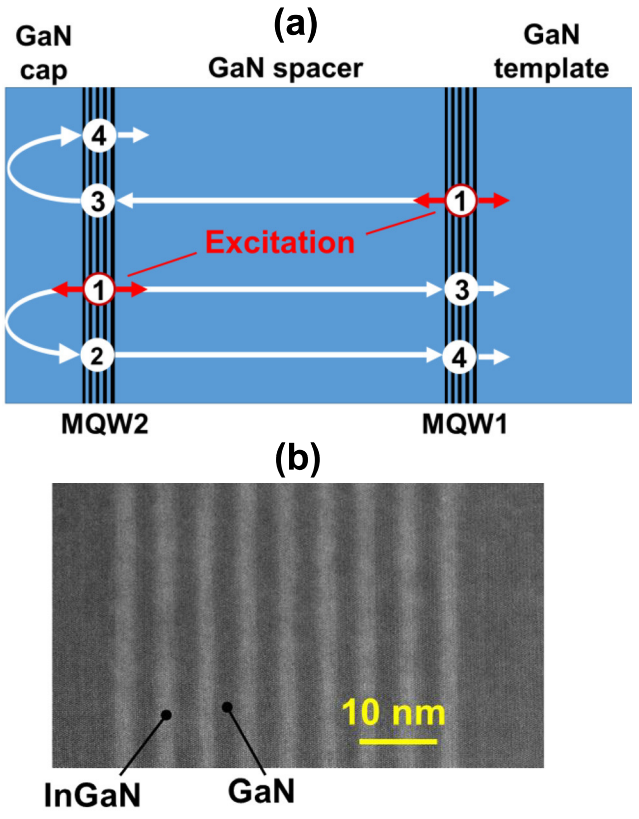

FIG. 2. (a) Schematic diagram of the sample structure, with arrows indicating the propagation paths of acoustic wavepackets generated by the optical excitation of MQW structures. The numbers indicate subsequent points in time when acoustic wavepackets propagate through MQWs and are detected by the probe beam. (b) STEM image of the top superlattice structure (MQW2) of sample 2.

Figure 3(a) shows the dependence of the measured probe beam transmission on the time delay dominated by the electronic response; subtracting the slow background reveals acoustic oscillations shown in Figs. 3(b)–3(d). A Fourier transform (FT) reveals an acoustic frequency of 1.06 THz [see Figs. 3(e) and 3(f)]. Mechanisms of the laser generation and detection of acoustic waves in InGaN/GaN MQW structures have been described in detail previously.[38] The excitation pulse generates free carriers which screen the electric field associated with the static stress in the piezoelectric MQW structure. The rapid change in the electric field, through the inverse piezoelectric effect, yields a driving force that initiates coherent phonon oscillations. The acoustic waves modulate the effective optical constants of the MQW structure, resulting in the oscillations in the transmission of the probe beam.[38] The initial acoustic signal labeled "1" and shown in detail in Fig. 3(c) is similar to what was previously observed in many pump-probe experiments on InGaN/GaN MQWs,[14,18,19,38] the only difference being that the signal is generated simultaneously in two MQW structures.

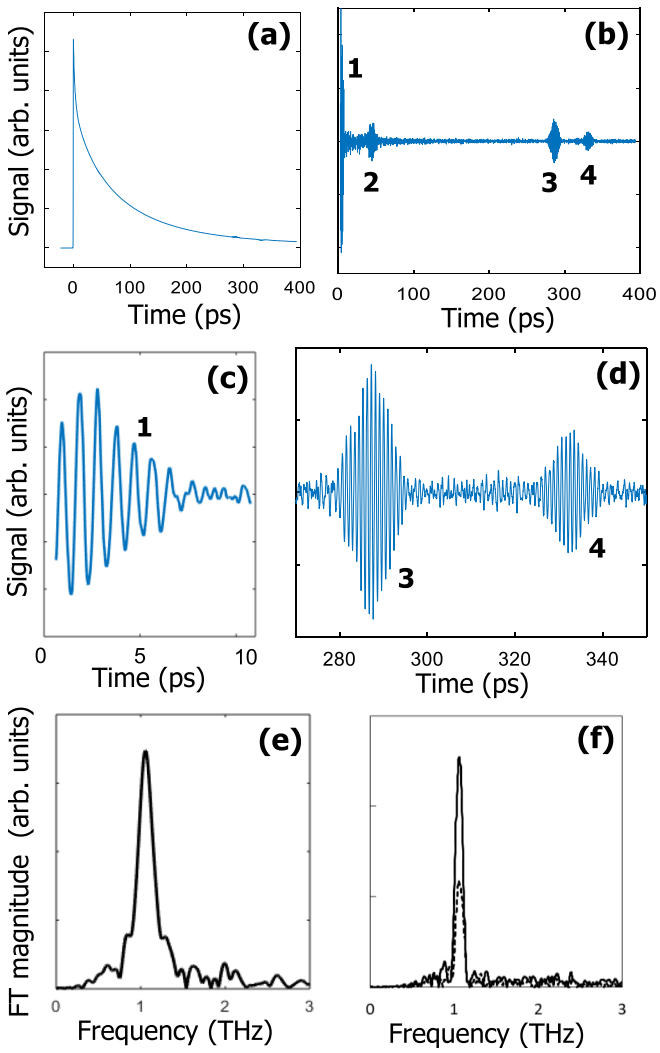

FIG. 3. Results from sample 1: (a) Raw signal waveform (transmitted probe intensity vs delay time). (b) Acoustic signal made more prominent by subtracting the slow background; the observed tone-bursts are numbered to correspond to the numbers in Fig. 2(a). (c) The initial acoustic signal. (d) Acoustic arrivals at large delays. (e) Fourier spectrum of the initial acoustic signal shown in (c). (f) Fourier spectrum of the delayed tone-bursts shown in (d), with solid and dashed lines corresponding to tone-bursts 3 and 4, respectively.

Each MQW structure generates two counter-propagating acoustic wavepackets with a rectangular envelope, the number of acoustic periods in each wavepacket being equal to the number of MQW periods. The oscillations in the transmitted probe intensity are observed as long as the wavepackets are propagating through the MQW structure; as soon as they are out of the MQW, the oscillating signal disappears. The acoustic oscillations in the signal reappear whenever an acoustic wavepacket again enters a MQW structure. Figure 3(b) reveals three distinct tone-bursts (2–4) following the initial acoustic response. The origin of these tone-bursts is schematically explained in Fig. 2(a). The first delayed tone-burst (2) is observed when a wavepacket generated by MQW2 returns to MQW2 after reflection from the free surface. The next tone-burst (3) is observed at a large delay of ∼290 ps, corresponding to the GaN spacer thickness divided by the speed of sound along the c-axis of GaN equal to 8020 m/s.[39] It is produced by a wavepacket generated by MQW1 passing through MQW2 after having crossed the spacer layer, and, simultaneously, by a wavepacket generated by MQW2 passing through MQW1. As can be seen in Fig. 3(d), the tone burst has a triangular envelope resulting from the convolution of the rectangular envelope of the phonon wavepacket and the rectangular envelope of the MQW profile. The last tone-burst is additionally delayed by ∼45 ps: the wavepacket generated by MQW1, after crossing the spacer and propagating through MQW2, crosses the GaN cap layer, reflects from the free surface, and returns to MQW2, with an additional delay corresponding to a double thickness of the cap layer plus the MQW thickness. Simultaneously, the wavepacket initially launched from MQW2 in the direction of the surface arrives to MQW1 with the same additional delay. Thus, delayed tone bursts 3 and 4 are produced simultaneously by two wavepackets passing through both MQW structures.

The amplitude of tone-burst 4 is smaller primarily due to losses associated with reflection from the free surface.[7] The squared ratio of the amplitudes of the two tone-bursts equal to 0.21 [as determined from the magnitudes of the Fourier-transform peaks in Fig. 3(f)] provides a lower bound estimate of the surface specularity; the second tone burst may be additionally attenuated by a double pass through the GaN cap layer and a pass through an MQW structure which involves crossing 18 GaN-InGaN interfaces. However, scattering losses at GaN-InGaN interfaces are likely to be small due to the very small differences in acoustic impedances and velocities.[19]

Figure 4(a) presents the delayed signals from sample 2. Since the MQW period for this sample is smaller, it yields a higher acoustic frequency of 1.39 THz, as can be seen in Fig. 4(b). The signal waveform is somewhat noisier, but the second wavepacket is still present, indicating that a partial specular reflection from the surface is still observed at this very high frequency.

We quantify the losses associated with the propagation through the GaN spacer by comparing the amplitudes of the initial signal, such as the signal shown in Fig. 3(c), and of the delayed tone-burst 3. In the absence of losses, the amplitude of the delayed wavepacket should be equal to 1/2 of the oscillation amplitude in the initial signal (because each MQW launches two wavepackets propagating in opposite

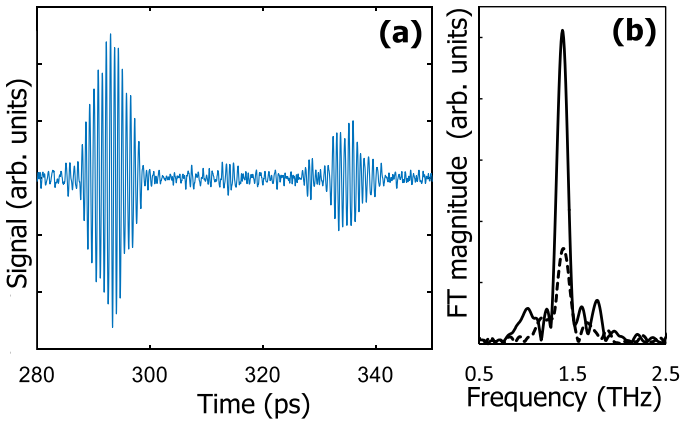

FIG. 4. Results from sample 2: (a) delayed acoustic arrivals (slow background subtracted); (b) Fourier spectra of the first (solid line) and second (dashed line) wavepackets in (a).

directions and the initial signal is produced by both wavepackets). On the other hand, the delayed signal is twice as long as the initial tone-burst; as a result, in the ideal case without losses, the height of the FT peak should be exactly the same for the initial and delayed signals. Thus, the attenuation of the acoustic amplitude is given by the ratio of the FT peak magnitudes A_3/A_1. If the observed attenuation comes solely from the propagation loss in the GaN spacer, it is given by

$$\frac{A_3}{A_1} = \exp\left(-\frac{T_d}{2\tau}\right), \tag{1}$$

where T_d is the wavepacket propagation time equal to the observed time delay and τ is the phonon lifetime. The factor 1/2 in the exponent comes from the fact that the common definition of the phonon lifetime corresponds to 1/e decay for the energy rather than for the amplitude. Thus, the phonon lifetime can be obtained from the measured ratio A_3/A_1. Measurements at six different points on sample 1 yielded a lifetime of 136 ± 20 ps, whereas measurements at 5 points on sample 2 yielded 55 ± 7 ps.

As can be seen in Fig. 1, the experimental lifetimes are significantly smaller than the calculated values. We believe that the measured attenuation may be affected by the non-uniformity of the GaN spacer thickness within the probe laser spot. If we assume that the spacer thickness L varies randomly within the laser spot, then the reduction in the observed signal amplitude is given by averaging $\exp(ikL)$, where k is the phonon wavevector, over the distribution of L. For a Gaussian distribution, averaging yields the apparent amplitude attenuation given by

$$\frac{A_3}{A_1} = \exp\left(-\frac{k^2\sigma^2}{2}\right), \tag{2}$$

where σ is the rms deviation of the thickness L from the average value. If we assume that the observed attenuation comes entirely from the thickness nonuniformity, Eq. (2) yields $\sigma = 1.9$ nm for sample 1 and 2.1 nm for sample 2. Considering that the total thickness is 2.3 μm, non-uniformity of 2 nm within the laser spot does not appear unlikely. The observed point-to-point variability of the measured lifetimes also indicates the likely role of the thickness non-uniformity.

Thus, the phonon lifetimes determined from the measured attenuation of the delayed signals should be considered lower bounds; further investigation is required to separate the intrinsic phonon attenuation from extrinsic factors such as GaN thickness non-uniformity. Still, even with our lower bound estimate for the phonon lifetime at 1.06 THz, we obtain a material Q-factor, i.e., the product of the phonon lifetime and the angular frequency, of 905, which is only two times smaller than that previously reported at 1.2 GHz.[25] The product of the quality factor and frequency $f \times Q$, which is often used as a performance metric for acousto-electronic materials,[22,25] comes out at 9.7×10^{14} Hz, which is about 400 times higher than the highest room temperature value for GaN measured in the GHz range.[25]

In conclusion, we observed the propagation of 1–1.4 THz coherent longitudinal acoustic phonons in GaN at room temperature over a distance exceeding 2 μm using two MQW structures serving as both transducers and receivers. Our results yielded lower bounds for room temperature phonon lifetimes in GaN. In particular, the lower bound for the material Q-factor at 1 THz is found to be only two times smaller than the Q-factor reported at 1.2 GHz. Thus, intrinsic losses do not pose an obstacle for expanding the frequency range of acousto-electronic devices all the way to THz frequencies. We also observed a partial specular reflection from the surface at 1.4 THz. The results show the potential for experiments with coherent phonon wave packets at frequencies comparable to those of heat-carrying thermal phonons, which have hitherto only been possible with molecular dynamics simulations.[2–4]

The contribution by A.A.M., H.D.S., and K.A.N. was supported by the U.S. Department of Energy, Office of Basic Energy Sciences under Award No. DE-FG02-00ER15087. The contribution by T.-C.H., Y.-T.Y., T.-H. C., and C.-K.S. was supported by the Taiwan Ministry of Science and Technology, MOST 106-2112-M-002-004-MY3. The contribution by J.S.G., D.W.S., R.L.F., and A.B. was supported by the University of Houston Grants to Enhance Research Program (Grant No. 55322). L.L. acknowledges support from the U. S. Department of Energy, Office of Science, Office of Basic Energy Sciences, Materials Sciences and Engineering Division. STEM imaging was conducted at the Center for Nanophase Materials Sciences, which is a DOE Office of Science User Facility, at Oak Ridge National Laboratory.

[1]D. G. Cahill, P. V. Braun, G. Chen, D. R. Clarke, S. Fan, K. E. Goodson, P. Keblinski, W. P. King, G. D. Mahan, A. Majumdar, H. J. Maris, S. R. Phillpot, E. Pop, and L. Shi, Appl. Phys. Rev. **1**, 011305 (2014).

[2]P. K. Schelling, S. R. Phillpot, and P. Keblinski, Appl. Phys. Lett. **80**, 2484 (2002).
[3]Z. T. Tian, B. E. White, Jr., and Y. Sun, Appl. Phys. Lett. **96**, 263113 (2010).
[4]H. Han, L. G. Potyomina, A. A. Darinskii, S. Volz, and Y. A. Kosevich, Phys. Rev. B **89**, 180301 (2014).
[5]C. Thomsen, H. T. Grahn, H. J. Maris, and J. Tauc, Phys. Rev. B **34**, 4129 (1986).
[6]B. C. Daly, K. Kang, Y. Wang, and D. G. Cahill, Phys. Rev. B **80**, 174112 (2009).
[7]Y.-C. Wen, C.-L. Hsieh, K.-H. Lin, H.-P. Chen, S.-C. Chin, C.-L. Hsiao, Y.-T. Lin, C.-S. Chang, Y.-C. Chang, L.-W. Tu, and C.-K. Sun, Phys. Rev. Lett. **103**, 264301 (2009).
[8]J. Cuffe, O. Ristow, E. Chávez, A. Shchepetov, P.-O. Chapuis, F. Alzina, M. Hettich, M. Prunnila, J. Ahopelto, T. Dekorsy, and C. M. Sotomayor Torres, Phys. Rev. Lett. **110**, 095503 (2013).
[9]A. A. Maznev, F. Hofmann, A. Jandl, K. Esfarjani, M. T. Bulsara, E. A. Fitzgerald, G. Chen, and K. A. Nelson, Appl. Phys. Lett. **102**, 041901 (2013).
[10]B. Liao, A. A. Maznev, K. A. Nelson, and G. Chen, Nat. Commun. **7**, 13174 (2016).
[11]A notable exception is a very recent study, T. Henighan, M. Trigo, S. Bonetti, P. Granitzka, D. Higley, Z. Chen, M. P. Jiang, R. Kukreja, A. Gray, A. H. Reid, E. Jal, M. C. Hoffmann, M. Kozina, S. Song, M. Chollet, D. Zhu, P. F. Xu, J. Jeong, K. Carva, P. Maldonado, P. M. Oppeneer, M. G. Samant, S. S. P. Parkin, D. A. Reis, and H. A. Dürr, Phys. Rev. B **93**, 220301 (2016). In this work, frequency components of an acoustic pulse up to 3.5 THz were detected in an iron film using time-resolved femtosecond x-ray scattering. The coherent phonons were detected in the same film where they were generated, with no transmission or reflection through/from an interface involved. Nevertheless, the surface of the epitaxially grown single crystal Fe film where the acoustic pulse was generated must have been nearly atomically flat.
[12]A. Yamamoto, T. Mishina, Y. Masumoto, and M. Nakayama, Phys. Rev. Lett. **73**, 740 (1994).
[13]A. Bartels, T. Dekorsy, H. Kurz, and K. Köhler, Phys. Rev. Lett. **82**, 1044 (1999).
[14]C.-K. Sun, J.-C. Liang, and X.-Y. Yu, Phys. Rev. Lett. **84**, 179 (2000).
[15]A. Huynh, B. Perrin, B. Jusserand, and A. Lemaître, Appl. Phys. Lett. **99**, 191908 (2011).
[16]A. Huynh, B. Perrin, and A. Lemaître, Ultrasonics **56**, 66 (2015).
[17]R. Legrand, A. Huynh, B. Jusserand, B. Perrin, and A. Lemaître, Phys. Rev. B **93**, 184304 (2016).
[18]G.-W. Chern, K.-H. Lin, Y.-K. Huang, and C.-K. Sun, Phys. Rev. B **67**, 121303 (2003).
[19]A. A. Maznev, K. J. Manke, K.-H. Lin, K. A. Nelson, C.-K. Sun, and J.-I. Chyi, Ultrasonics **52**, 1 (2012).
[20]J. Cho, Z. Li, E. Bozorg-Grayeli, T. Kodama, D. Francis, F. Ejeckam, F. Faili, M. Asheghi, and K. E. Goodson, IEEE Trans. Compon. Packag. Manuf. Technol. **3**, 79 (2013).
[21]Z. Yan, G. Liu, J. M. Khan, and A. A. Balandin, Nat. Commun. **3**, 827 (2012).
[22]M. Rais-Zadeh, V. J. Gokhale, A. Ansari, M. Faucher, D. Théron, Y. Cordier, and L. Buchaillot, J. Microelectromech. Syst. **23**, 1252 (2014).
[23]D. A. Pinnow, IEEE J. Quantum Electron. **6**, 223 (1970).
[24]B. G. Helme and P. J. King, Phys. Status Solidi (a) **45**, K33 (1978).
[25]L. C. Popa and D. Weinstein, in *Proceedings of the Joint European Frequency Time Forum International. Frequency Control Symposium* (EFTF/IFCS) (2013), p. 922.
[26]H. J. Maris, in *Physical Acoustics*, edited by W. P. Mason and R. N. Thurston (Academic, New York, 1971), Vol. 8, p. 279.
[27]P. A. Mante, Y. R. Huang, S. C. Yang, T. M. Liu, A. A. Maznev, J. K. Sheu, and C. K. Sun, Ultrasonics **56**, 52 (2015).
[28]D. A. Broido, M. Malorny, G. Birner, N. Mingo, and D. A. Stewart, Appl. Phys. Lett. **91**, 231922 (2007).
[29]K. Esfarjani, G. Chen, and H. Stokes, Phys. Rev. B **84**, 085204 (2011).
[30]L. Lindsay, D. A. Broido, and T. L. Reinecke, Phys. Rev. Lett. **109**, 095901 (2012).
[31]A. Debernardi, S. Baroni, and E. Molinari, Phys. Rev. Lett. **75**, 1819 (1995).
[32]G. Deinzer, G. Birner, and D. Strauch, Phys. Rev. B **67**, 144304 (2003).
[33]N. Bonini, M. Lazzeri, N. Marzari, and F. Mauri, Phys. Rev. Lett. **99**, 176802 (2007).
[34]P. Hohenberg and W. Kohn, Phys. Rev. **136**, B864 (1964).
[35]W. Kohn and L. J. Sham, Phys. Rev. **140**, A1133 (1965).
[36]J. M. Ziman, *Electrons and Phonons* (Oxford University Press, London, 1960), p. 298.
[37]C. Boney, D. Starikov, I. Hernandez, R. Pillai, and A. Bensaoula, J. Vac. Sci. Technol. B **29**, 03C106 (2011).
[38]G.-W. Chern, K.-H. Lin, and C.-K. Sun, J. Appl. Phys. **95**, 1114 (2004).
[39]C. Deger, E. Born, H. Angerer, O. Ambacher, M. Stutzmann, J. Hornsteiner, E. Riha, and G. Fischerauer, Appl. Phys. Lett. **72**, 2400 (1998).